299
8

Bowing of marble panels: on-site damage analysis from the Oeconomicum Building at Göttingen (Germany)

A. KOCH & S. SIEGESMUND

Geowissenschaftliches Zentrum der Universität Göttingen, Goldschmidtstrasse 3, D-37077 Göttingen, Germany (e-mail: akoch4@gwdg.de)

Abstract: The use of natural stone panels or cladding material for building facades has led to some durability problems, especially with marble slabs. To examine the effects of intrinsic and extrinsic parameters on bowing, a very detailed study was performed on the Oeconomicum Building at the University of Goettingen. In total 1556 panels from the whole building were measured with respect to bowing using a bow-meter. The variation of bowing ranges from concave (up to 23 mm/m) to convex (up to −11 mm/m). The variation is not controlled by the position with respect to the geographical coordinates, height above ground, shadows, temperature etc. On the north facade the different rock structures visible on the panel surfaces are a result of the marble slabs being cut in different directions. The different degrees of bowing are associated with the structure of the marble since all other influencing factors are relatively constant (position, temperature, moisture content, building physics). Experimental data on the expansion behaviour under dry and/or wet conditions reveal different degrees of bowing with respect to the rock fabric and may help to explain the observed differences in bowing. The effect of the rock fabric, especially of the lattice preferred orientation in this case, clearly controls the deterioration of the marble and the degree of bowing. The bowing is also characterized by an increase in the porosity, decreasing values of ultrasonic wave velocities and flexural strength. The loss of cohesion in the strongly deteriorated panels is clearly visible in the microstructure by the open grain boundaries which are interconnected to intergranular microcracks.

Marbles and limestones exhibit a large variation in the way they weather including back-weathering, micro-karst, breakouts, coloration, formation of crusts, biological colonization, granular desintegration and flaking. In recent times, relatively thin slabs have been used for complete facades on commercial buildings in contrast to the more traditional thick stone facings. New developments in cutting machinery allow the design of slabs up to 15 mm thick. The most spectacular deterioration feature of these marble slabs is their bowing behaviour. Such phenomena, however, are well known from ancient grave stones (Grimm 1994, 1999). The now completely replaced facade cladding of Finlandia Hall in Helsinki (Ritter 1992) or the Amoco Building in Chicago (Trewitt & Tuchmann 1998), both made of Carrara marble, are often cited as examples. Presently, the Grand Arche de la Defense in Paris is under reconstruction due to fixing problems resulting from the bowing of stone panels.

Logan *et al.* (1993) explained the bowing of marble slabs on the Amoco Building as being due to the anomalous expansion–contraction behaviour of calcite combined with the release of locked residual stresses based on laboratory testing. The hypotheses of other researchers have required the presence of moisture or gravity variation (Bucher 1956; Bortz *et al.* 1988; Winkler 1994). However, all the existing explanations can be regarded as being due to intrinsic and extrinsic properties. The extrinsic properties include temperature, moisture, freeze–thaw cycles, environmental factors, conservation or cleaning effects, anchoring or fixing systems, joint widths, dimension and thickness of slabs. The intrinsic properties of the stone are determined by the mineralogical composition and the rock fabric (i.e. grain size, grain boundary configuration, shape and lattice preferred orientation as well as the microcrack fabric). These intrinsic properties control the mechanical and physical properties such as porosity, permeability, Young's modulus, compressive, tensile and flexural strength, thermal expansion and thermal conductivity.

To help in understanding the mechanical weathering of marble, a very detailed study on bowed marble panels was performed at the Oeconomicum Building of the University of Goettingen (Fig. 1). Different approaches were applied for the characterization of the type and degree of bowing. All panels were inspected with a bow-meter (Fig. 2) to determine the intensity of bowing with respect to the geometry

From: SIEGESMUND, S., WEISS, T. & VOLLBRECHT, A. 2002. *Natural Stone, Weathering Phenomena, Conservation Strategies and Case Studies*. Geological Society, London, Special Publications, **205**, 299–314.
0305-8719/02/$15.00

Fig. 1. Representative part of the Oeconomicum Building (western part, north facade).

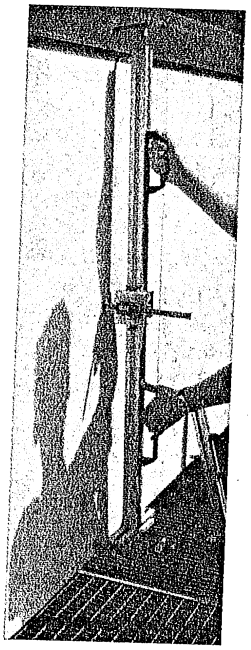

Fig. 2. Aluminium bridge (bow-meter) for measuring the bowing along the vertical centre line of the stone panels.

and physics of the building. Demounted panels were analysed in more detail in the laboratory; tests performed included mineralogical, fabric and petrophysical studies. Field studies suggest that bowing is also controlled by the rock structure, therefore emphasis was placed on the relationship between rock fabric, loss in strength and the type of bowing.

Building characteristics

The Oeconomicum Building at the University of Goettingen was built in 1966. The three-storied rectangular building has a length of 83 m in the north–south direction and a width of 55 m in the east–west direction with a height of 13 m. All facades are clad with panels of a white to dark strongly decorated marble (Peccia; see Fig. 1) of identical dimensions (length 128 cm, width 67 cm and thickness 3 cm). Each elevation has four rows of panels with windows in between (height 180 cm), each with a row of ventilation ducts (height 50 cm) above. Looking from the left to the right all panels were combined into groups of four except the outermost ones. The facades are interrupted only at two doors in the lowermost rows. The number of panels is 312 on the south facade, 308 on the north facade, 472 on the west facade and 464 on the east facade. In total 1556 marble panels were used as ornamentation on the building, corresponding to a total area of 1300 m^2. The open joint width between the panels was

originally 5 mm, but has now decreased to 0–3 mm; the joints were not filled with any kind of sealant.

The slabs are mounted with a kerf on a continuous rail at the bottom and are held by a 'ledge' at the top. There are no other mechanical anchoring or fixing systems. The cladding is ventilated with a cavity gap of 1–2 cm between the panels and the ferroconcrete structure.

Surrounding trees shelter parts of the facade. Some medium to large trees approximately 10 m high shade parts of the lower two rows on the east facade in the early morning. A similar situation is observed on the west facade where the shading of the trees influences the lower rows during the late afternoon in summer. On the south facade approximately half of the lower two rows are shaded by trees as well as parts of the third row. Some areas are permanently sheltered. The shading has occurred only in the recent past since the trees are quite young.

The original honed surface of the panels is still preserved except on parts of the lowermost rows where graffiti has been removed.

Goettingen is situated 167 m above sea level and features a climate typical for central Europe. The minimum monthly average temperature is 0°C in January and the maximum is 17°C in July. The average rainfall is 700 mm/a with a monthly average of at least 40 mm/month.

Experimental

To investigate the bowing phenomena of facade panels, systematic examinations of the cladding were carried out, along with detailed mapping of the cladding. Slabs from the building were demounted for further investigations to understand the mineralogy, rock fabric and important petrophysical properties with respect to the bowing.

The amount of bowing of each single panel was measured by an aluminium measuring bridge (bow-meter) with two supporting mounts, one with two legs, the other with one supporting leg ensuring stability (Fig. 2). The measuring bridge is equipped with a ruler fixed lengthways so that the distance between two supporting points is adjustable and measurable. To measure the bowing of one panel, the bow-meter is placed along the vertical centre line with support points at a distance of 1.20 m from each other and about 4 cm from the margin. A measuring mount including a vernier calliper is fixed concentrically between the support points. Before each measurement the vernier calliper was reset on a plane surface (for example a plate glass window). The bowing (B) of a panel is given as:

$$B = d / L \times 1000 \times a$$

where d (mm) is the measured value, L (mm) is the distance between two support points and a is a correction factor of 1.1. Positive values indicate concave and negative values convex bowing. Since all areas of a panel do not bow equally, the question arises as to how the degree of bowing is to be measured. A direct comparison of the results obtained from 50 panels where both vertical and diagonal measurements were recorded gives an empirically determined correlation factor of 1.1 between these different approaches (Fig. 3). Based on this correlation factor, all data are presented as diagonal measurements.

The character of the bowing was determined on four demounted panels using an orthogonal net with dimensions of 1.1 m × 0.6 m or 1 m × 0.6 m, respectively; measurements were taken every 10 cm to evaluate the small-scale geometry of bowing. The results are given as isolines illustrating lines of equal degree in bowing. In addition, at each of these points the ultrasonic wave velocities (V_p) was also measured.

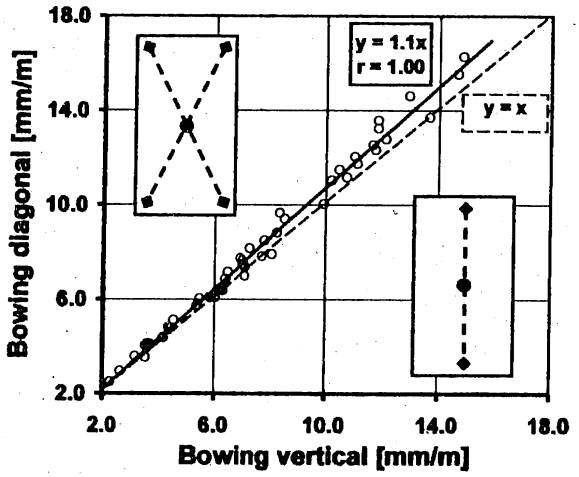

Fig. 3. Correlation between diagonal and vertical measurements, determined on 50 panels with a broad variation in bowing. The solid line represents the regression line, where r equals the correlation coefficient. The dashed line represents the perfect conformity of both measurements and is given for comparison only. The sketches illustrate the two different kinds of measurements and are each related to the corresponding axis. Diagonal bowing is determined as the median of two diagonal measurements per panel.

The temperature data of the panel surfaces were measured with a Raytek® Raynger ST 60 infrared thermometer. The porosity of representative samples from each panel representing different degrees of bowing was determined by a standard weighting method. The permeability of cylindrical samples was measured by the transient method using air as a flow medium. The gas pressure was kept constant at 0.5 MPa on one side of the sample. The determination of the flexural strength has been carried out in accordance with the standard EN 12372 (1999) on rectangular samples of 180 mm × 50 mm × 30 mm in two different directions orthogonal to the panel edges.

The mineralogy and fabric data were evaluated on orthogonal thin sections which were cut parallel to the macroscopic structures. To determine the texture, neutron diffraction was applied. The pole figure measurements were carried out at the time-of-flight neutron diffractometer NSHR, which is located at the pulsed reactor IBR-2 of the Frank Laboratory for Neutron Physics of the Joint Institute of Nuclear Research at Dubna (Russia) (Walther *et al.* 1995; Ullemeyer *et al.* 1998).

Results

The cladding material at the Oeconomicum Building is a coarse-grained Peccia marble ('Cristallino Virginio') from Switzerland. It consists mostly of a dark to white, sometimes light whitish calcitic matrix which is transected by brownish biotite veins or greyish graphite veins. These veins appear in a millimetre to centimetre scale, sometimes in a decimetre scale or they may be completely absent. The panels without any visible structures are homogenous and white in colour. The veins define the foliation as well as light white millimetre to centimetre thick elongated lenses or coarser-grained calcitic veins. The dark veins are sometimes folded, which is often observed at the panels from the north facade (see Fig. 1). All other claddings show a more or less visible foliation.

Most of the panels exhibit a remarkable concave bowing (Fig. 4a). Depending on the amount of bowing, panels may show cracks in the upper corners (Fig. 4b) up to 15 cm long as well as cracks at the junction with the kerf (Fig. 4c). At an advanced stage of deterioration these cracks can become transformed into larger-scale breakouts.

As illustrated in Figure 5 the degree of bowing is different at each facade. Nearly all panels are bent concave except for the east facade where row 2 shows a clear convex bowing of about -6.8 ± 2.3 mm/m. Row 1 of the east facade is also almost totally convex, but much weaker with a mean value of -1.5 ± 1.1 mm/m. The same observation occurs at parts of the east facade (row 3) and at the north facade (row 1). All other panels show a more or less concave bowing with average row values of 1.3 ± 1.0 mm/m (south facade row 1) up to 15.6 ± 2.9 mm/m (east facade row 4). The maximum value for a single panel was also registered in the latter row at 23 mm/m. The east facade holds the maximum of both concave and

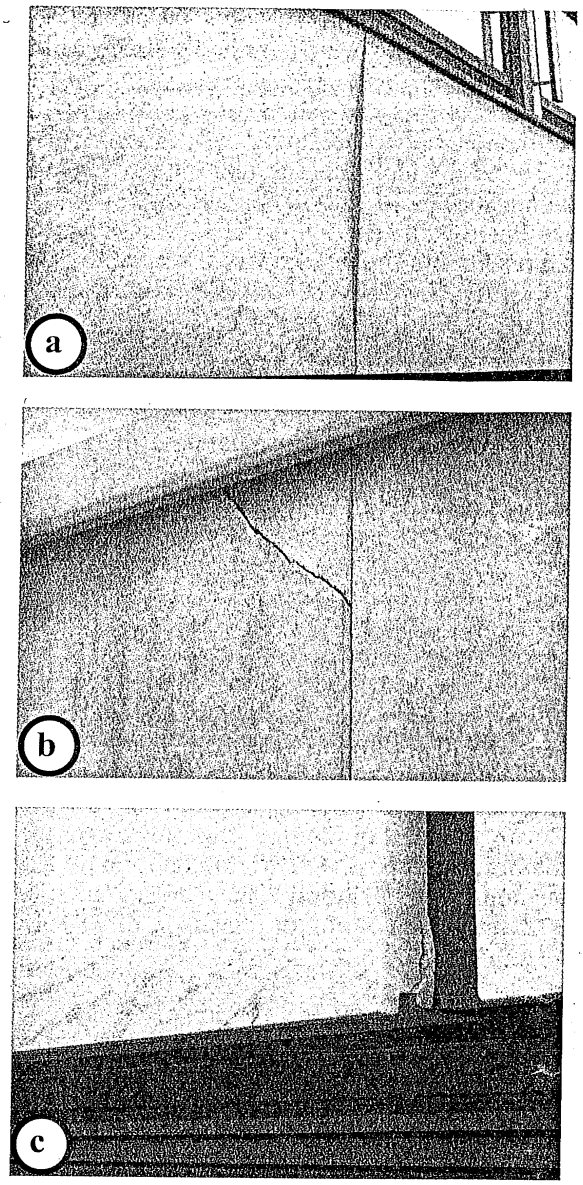

Fig. 4. Observed damage on the investigated marble panels. (**a**) Concave bowing (left panel). (**b**) Crack at the upper corner. (**c**) Crack initiated at the kerf.

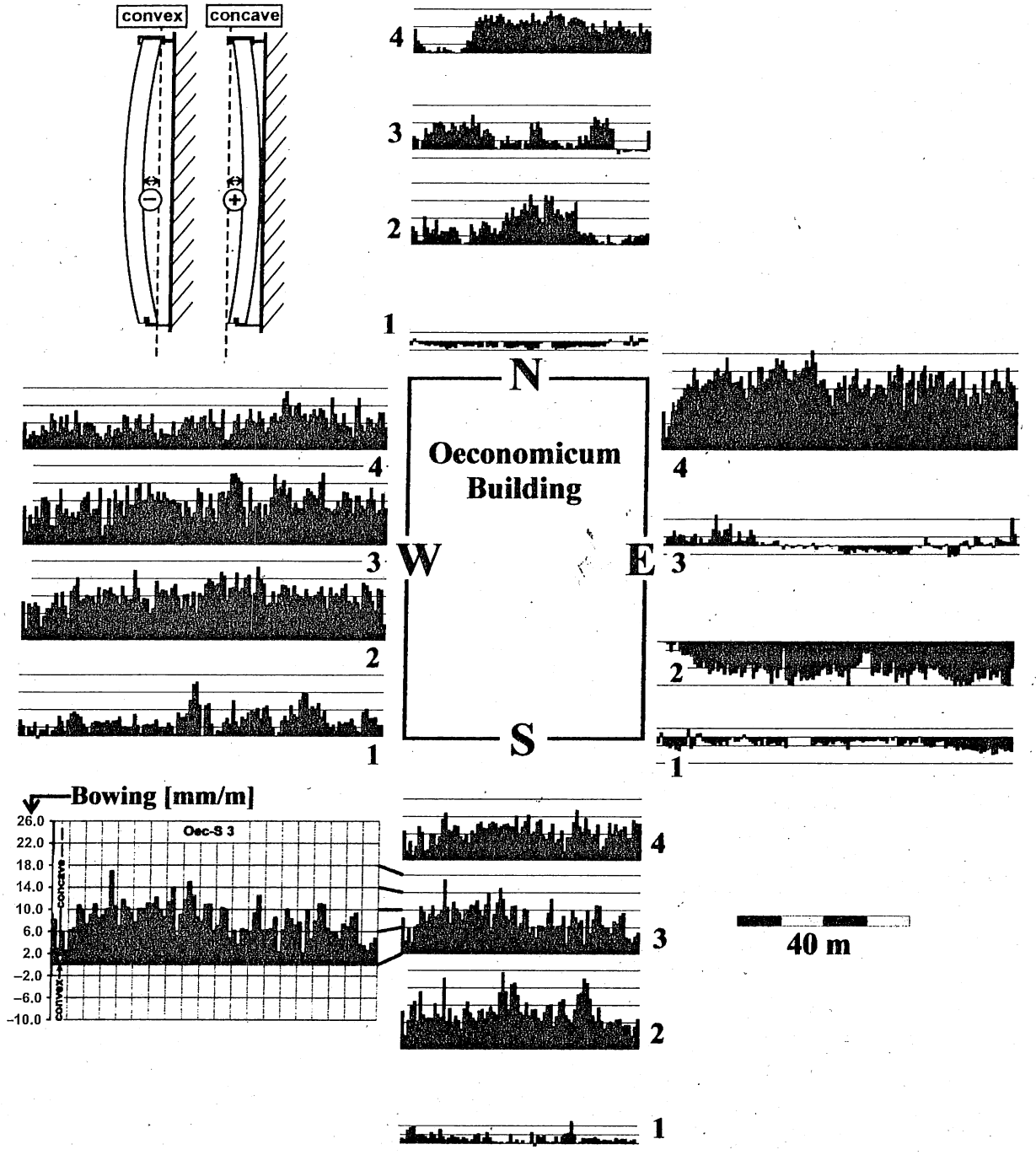

Fig. 5. Quantification of the bowing of all facade panels at the Oeconomicum Building depending on the orientation and the height. The histograms present the degree of bowing in the respective rows. As sketched at the upper left, positive values are equivalent to concave bowing and negative values are equivalent to convex bowing. To identify the amount of bowing by means of the height of the columns a complete diagram of row 3 (south facade) has been enlarged.

convex bowing (Fig. 5). In contrast, the west and south facades exhibit a more homogeneous distribution with a low mean bowing in the lowermost row (west facade: 3.7 ± 2.4 mm/m; south facade: 1.3 ± 1.0 mm/m) and a medium degree of bowing in rows 2–4 with mean values of 6–10 mm/m. The lowermost parts of each facade generally show the lowest values. The north facade exhibits comparable patterns with very weak convex bowing in row 1 and relatively weak concave ones in rows 2–4.

The bowing behaviour at the same height can

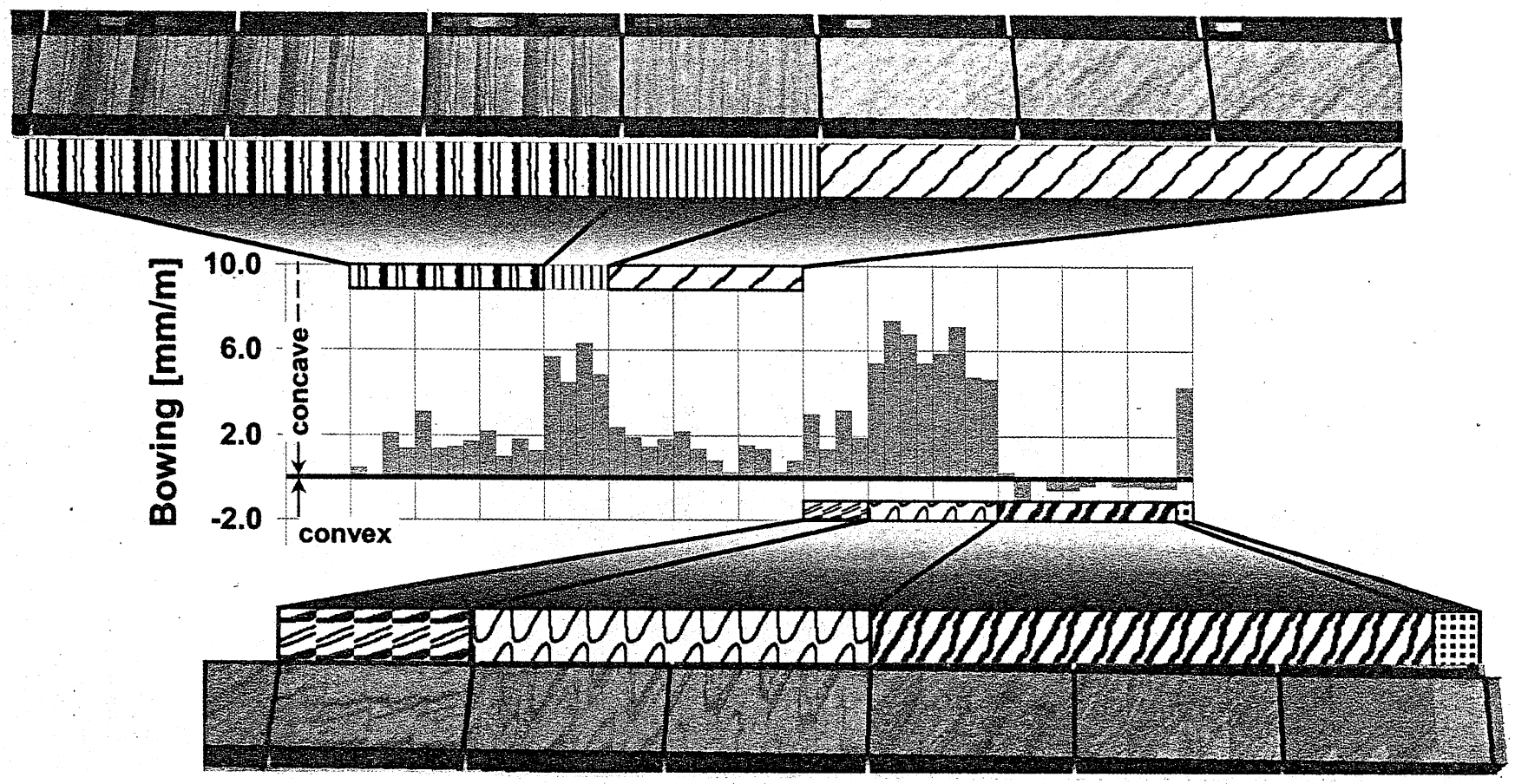

Fig. 6. Correlation between macrostructural fabric elements and bowing. The ornamental pattern of facade panels in the third row of the north facade is due to different block-cut directions and is also connected to different orientations of the foliation.

change from one group of panels to the next one. Very rarely is the bowing different from panel to panel within a single group. The macroscopically observed structure is more or less comparable for each single panel within each row of four panels. This means that the cutting direction, with respect to any metamorphic layering, foliation or macroscopic folds, was different for most of the groups. For aesthetic reasons the panels with identical ornamental or decorative elements, i.e. the same cutting direction, were arranged in such a way that panels with a comparable structure are combined together (Fig. 6; see also Fig. 1). Even if it is not yet known how the rock structure influences bowing, it is obvious from these findings that there is a causal connection between fabric anisotropies and the bowing of panels. Therefore, the close correlation between the fabric and the amount of bowing given in Figure 6 has to be considered without any doubt as a control on the deterioration mechanisms.

In order to illustrate the decay of stone panelling, detailed mapping of the building was found to be the most appropriate method (Fig. 7). Consequently, it is useful and necessary to distinguish different classes of deformation (Fig. 7). Figure 8 gives a first rough correlation between (a) an evaluated deformation class, and (b) the relative frequency of visible damage like cracks (length ≥10 cm) and breakouts (fracture ≥10 cm). From weak convex bowing (class −2: 1%) to strong concave bowing (class 5: 81%) an increase in cracking occurs. Furthermore, the ratio of panels showing both cracks and breakouts increases rapidly from class 3 (1%) to class 5 (31%).

Temperature is one of the main factors which may significantly influence the degree of bowing (Rosenholtz & Smith 1949; Sage 1988; Siegesmund *et al.* 2000). Measurements have been made at the panel surfaces to get an impression of how bowing is affected by temperature. Figure 9 illustrates the bowing surface temperature relationship measured on clear sunny days. Rows 1 and 2 of the south facade were investigated because these were areas where the highest expected temperatures would be influenced by different shadow impacts. The first dataset includes two different time periods (noon and afternoon) which takes into account moving shadows produced by trees. However, no significant difference in the range of temperature between the two rows can be observed. The temperature varies from 14 to 34°C at noon and from 21 to 32°C during the late afternoon, thus the differences in bowing between row 1 (1.3 ± 1.0 mm/m) and row 2 (8.7 ± 3.0 mm/m) cannot be explained exclusively by surface temperature. The temperature maximum in the middle of row 2 is in fact congruent with the bowing maximum.

To examine the effect of bowing on the mechanical and physical properties, as well as on the rock fabric, nine panels from different facades representing a broad variation of bowing were removed (Table 1). The panels were selected for their degree of deterioration: (a) panels with a low degree of bowing from sheltered places like the north facade; (b) panels with a medium degree of bowing exposed to the sun for part of the day and less sheltered places such as the west or east facade; and (c) panels with a high degree of bowing from very exposed locations like the south facade or, in one case, the uppermost row of the east facade (Table 1).

Porosity has been correlated with bowing and is demonstrated in Figure 10. Panels with a low degree of bowing show a porosity of 0.3% up to 0.7%. Strongly bowed panels have a porosity of up to 1.7%. Since the porosity has been measured in the panel centre it is possible that other parts of the panel have a much higher porosity. In conclusion it is obvious that the degree of bowing is correlated with an increase in the porosity.

A large scattering of the flexural strength (R_{tf}) is observed for weakly bowed panels with values 5.3 ± 0.5 MPa up to 13.4 ± 1.3 MPa (Fig. 11). The flexural strength decreases with an increase in bowing. In the medium to strongly bowed panels the strength variation is less pronounced with a range of 5.5 ± 0.2 MPa to 1.6 ± 0.2 MPa. In addition, the standard deviation of single values is significantly lower compared with panels of a high flexural strength (see error bars in Fig. 11).

The anisotropy of the flexural strength (A_{Rtf} (%) = $(R_{tf\,max} - R_{tf\,min})/R_{tf\,max} \times 100$) reaches values of up to 53%. The anisotropy of flexural strength depends on the orientation of the

Table 1. *Summary of the demounted panels*

Sample	Bowing (mm/m)		Facade	Row
L1	low	0.2	north	2
L2	low	0.0	north	2
L3	low	0.6	north	3
M1	medium	7.1	east	3
M2	medium	11.3	west	3
M3	medium	11.9	east	2
H1	high	17.1	south	3
H2	high	23.3	east	4
H3	high	25.6	sount	2

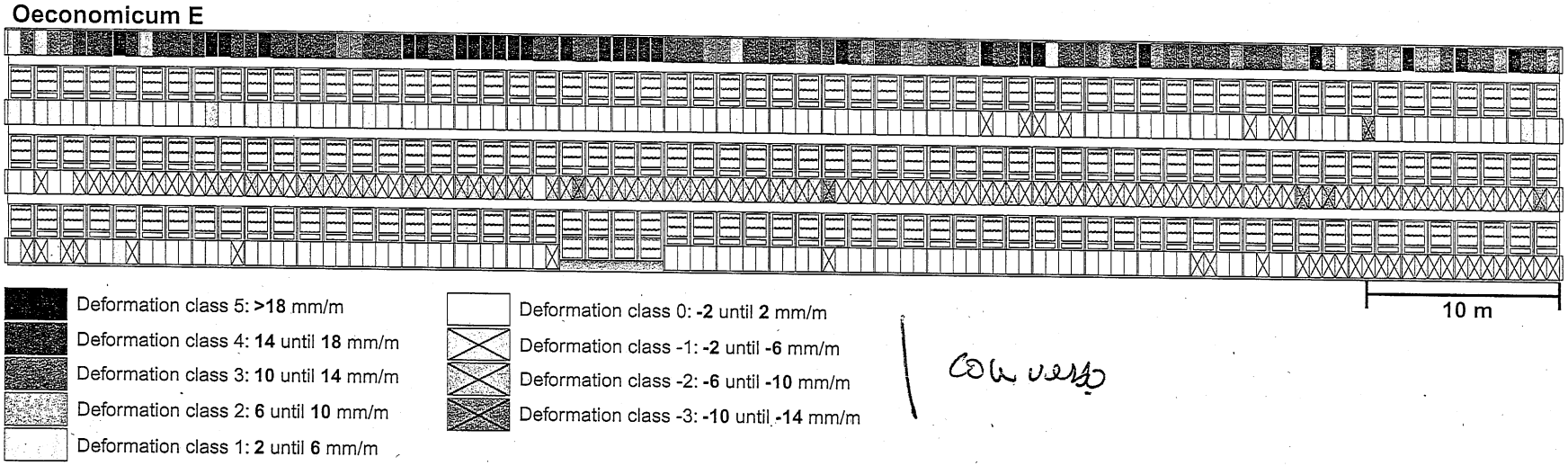

Fig. 7. Building map of the east facade of the Oeconomicum Building (true to scale) indicating the degree of deformation in the panels (compare with Fig. 5).

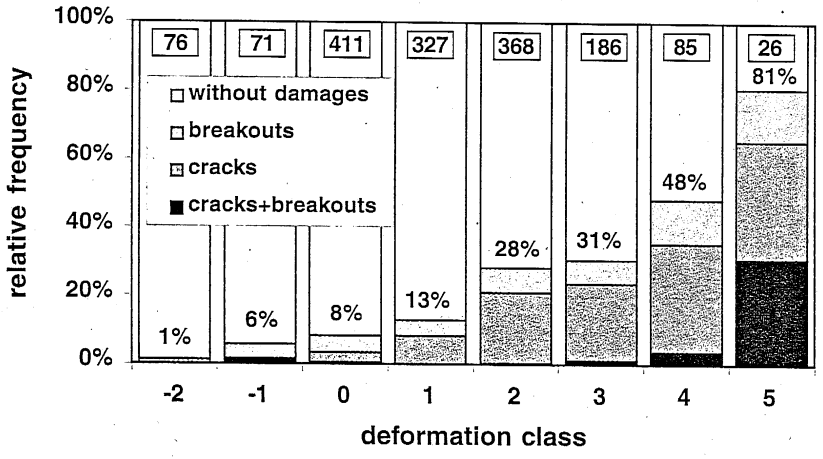

Fig. 8. Relative frequency of damaged panels depending on the deformation class. The absolute number of panels in each class is indicated at the top of the columns.

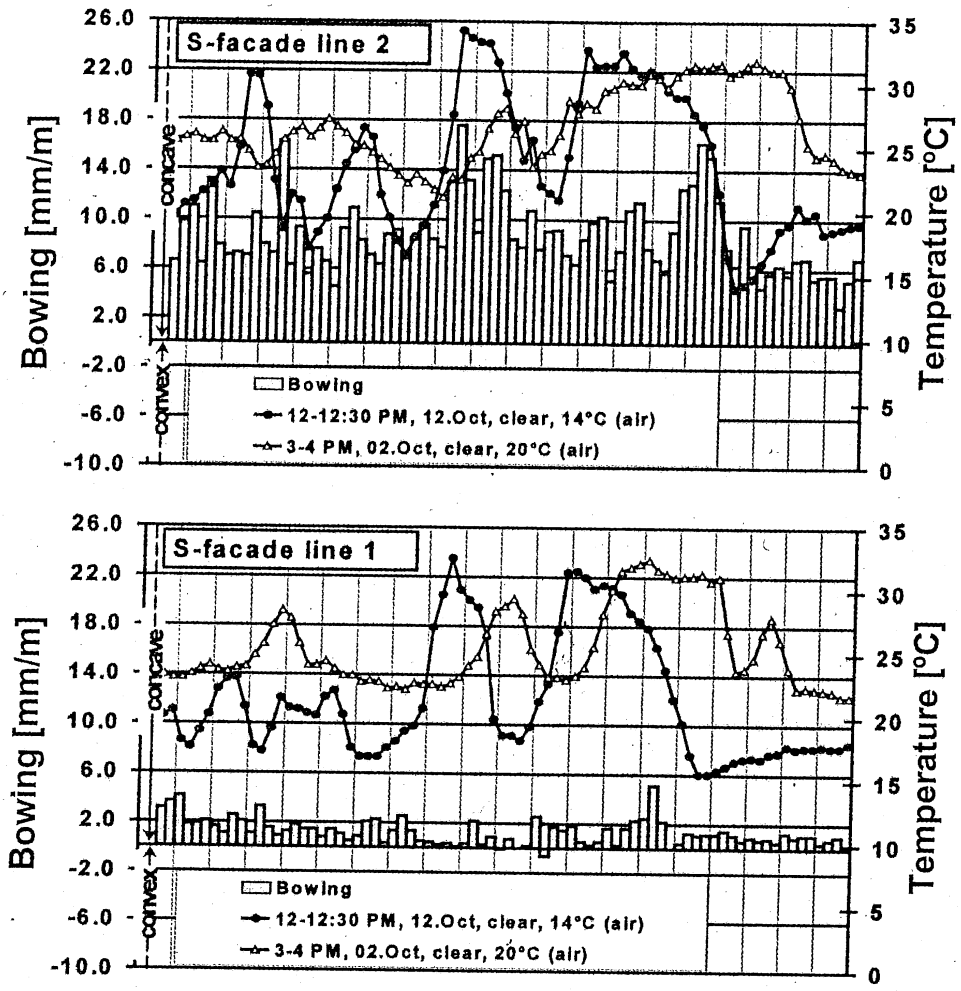

Fig. 9. Bowing surface temperature relationship of the lower two rows at the south facade.

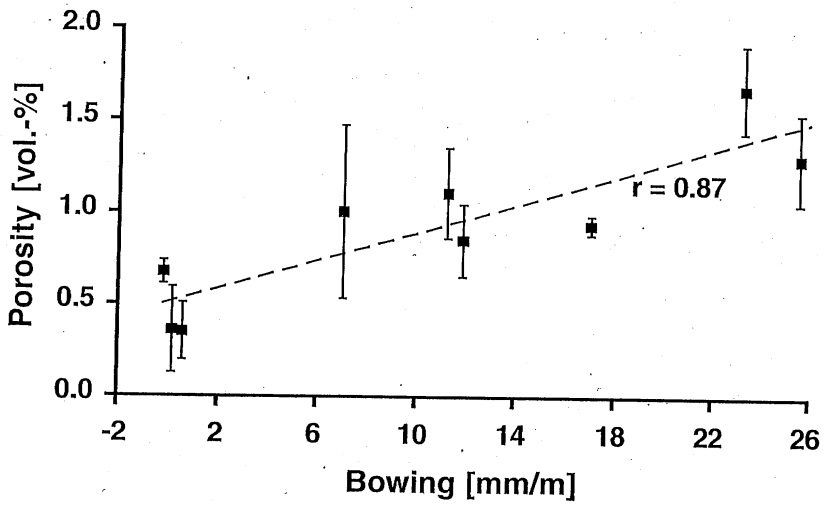

Fig. 10. Porosity of nine demounted panels depending on the degree of deformation (concave bowing). The standard deviations are indicated by error bars. The regression line (dashed) and the correlation coefficient (r) are given.

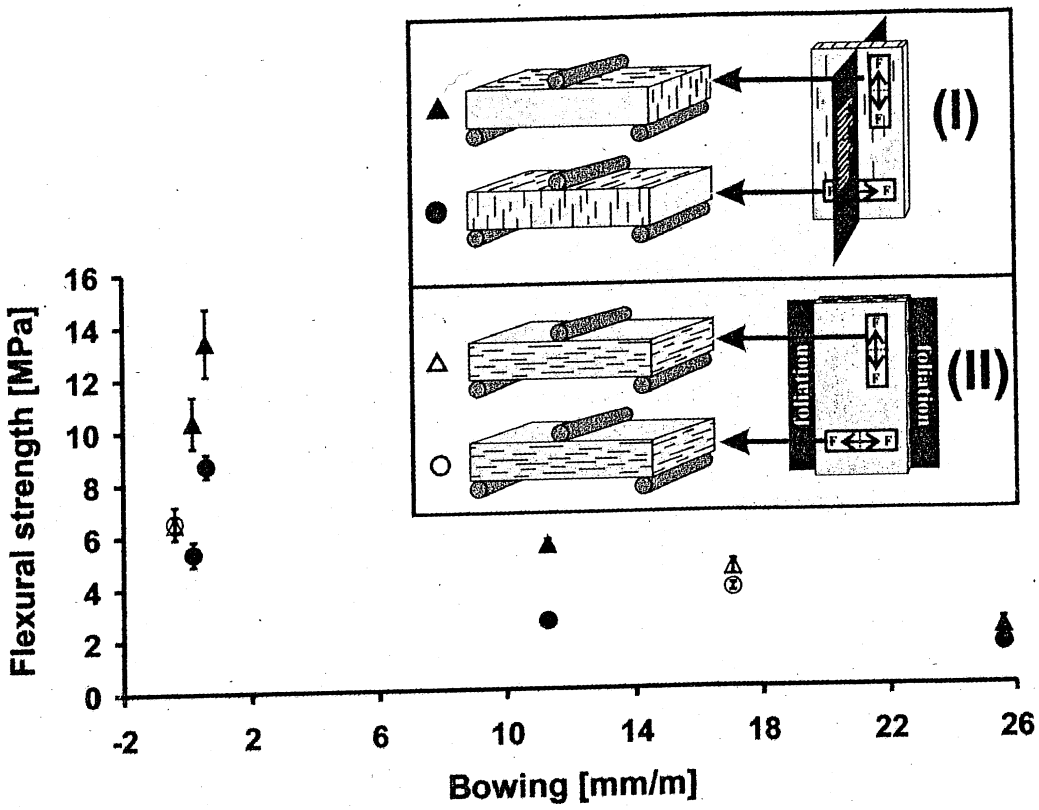

Fig. 11. Flexural strength of demounted panels depending on the degree of deformation (concave bowing). The values of flexural strength are given per panel in two directions of the vectored forces parallel to the panel edges. F equals force. The standard deviations are indicated by error bars.

foliation (see sketches in Fig. 11). The lowest values in strength are always observed where the direction of load is parallel to the foliation plane and where the resultant forces (F) are vectored perpendicular to the foliation (labelled as a solid circle in Fig. 11). In panels where the foliation is orientated as shown in sketch I of Figure 11, the flexural strength is reduced at least 30% in a direction where the resultant forces are vectored parallel to the short edge. In contrast, the panels with the smallest differences in flexural strength between two measured directions (anisotropies of 1% and 17%) show a foliation parallel to the panel surface (Fig. 11, sketch II), so that the resultant forces of the flexural strength are each measured parallel to the foliation plane.

The geometry of bowing for the most strongly deformed panels (H1, H2, H3, M2) is given in Figure 12. The V_p distribution is also illustrated, since ultrasonic measurements were often used as a non-destructive tool to quantify rock deterioration. This fact is based on the observation that the porosity and crack geometry control the reduction in velocity when progressively weathered (Weiss *et al.* 2002). All panels show a more or less symmetrical and homogeneous bowing. The isolines of equal bowing vary from a circular shape (Fig. 12a) to elliptical, where the ellipses can be elongated vertically (Fig. 12b,c) or horizontally (Fig. 12d). The most homogeneous distribution of the isolines in H1 (Fig. 12a) is recognized for panels where the surface is parallel to the foliation plane (compare with Fig. 11, sketch II), while a more elliptical distribution (Fig. 12b,d) is associated with a steeply inclined foliation with respect to the panel surface (compare with Fig. 11, sketch I). Looking at the V_p distributions (Fig. 12) two panels show relatively slow velocities in the range of 2.2–3.2 km/s (H1) and 1.7–3.1 km/s (H2). This is equivalent to a more highly deteriorated marble in the sense of Weiss *et al.* (2002). The distinctly higher velocities for M2 (3.6–4.5 km/s) and H3 (3.0–4.4 km/s) are measured parallel to the foliation (compare with Fig. 11, sketch I). The V_p minima of M2 and H3 are orientated parallel to the bowing maximum, while for H1 and H2 the pattern appears more complex.

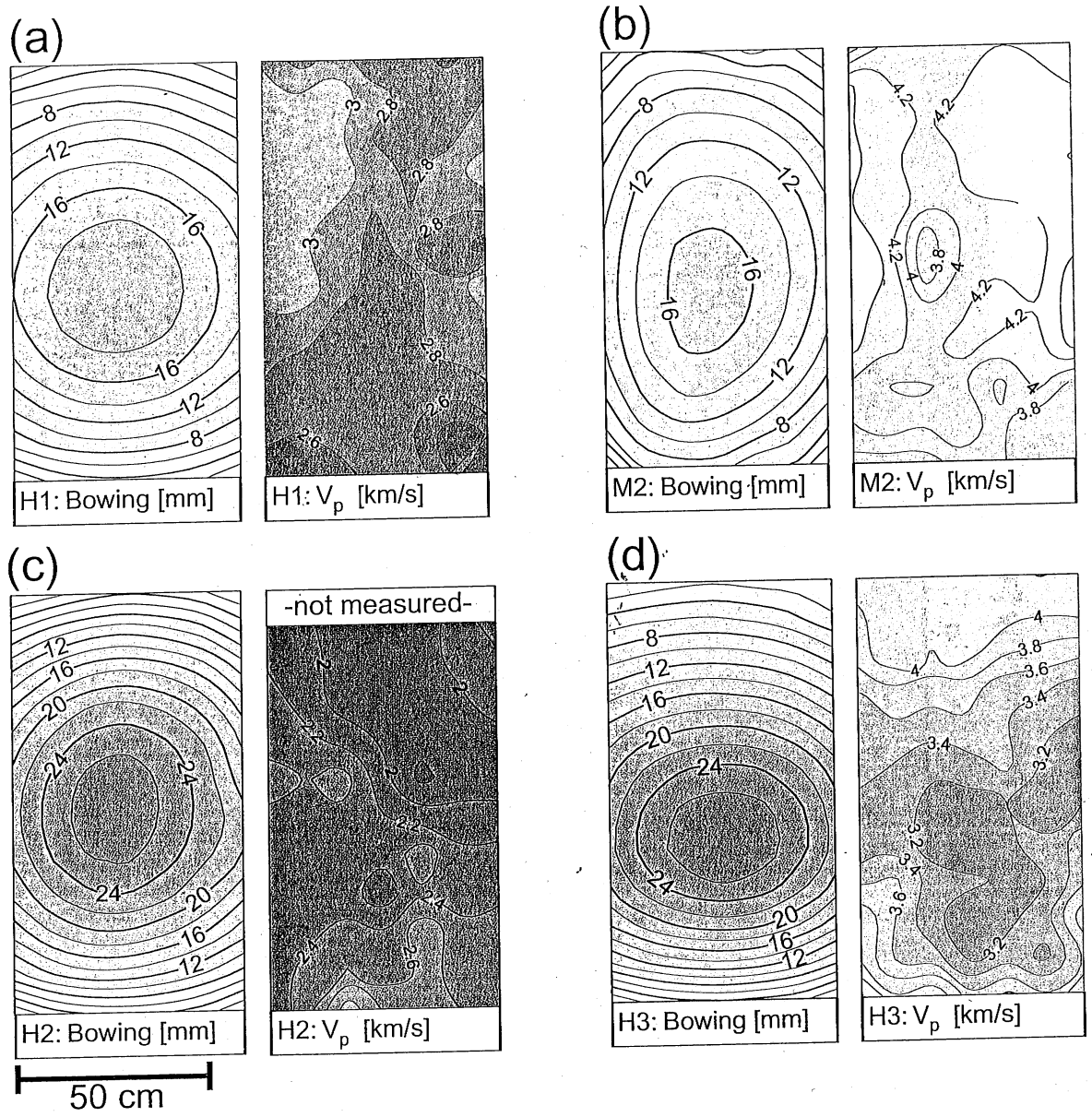

Fig. 12. Isoline pattern: bowing geometry versus V_p pattern. Dark grey indicates a strong bowing and a low V_p.

Two (H2, H3) of the four panels that feature the highest differences in V_p were also investigated with respect to their permeabilities to evaluate the interconnected pore space (Fig. 13a). A V_p minimum correlates with a maximum in air permeability. Comparing both panels it can be observed that H3 tends to higher values in permeability as well as in V_p corresponding to a measured direction parallel to the foliation. The behaviour of permeability across the different degrees of bowing of the panels is shown in Figure 13b. The permeability tends to increase with bowing, so a strong variation of permeability within single panels (H2 and H3) was found.

Discussion and conclusion

It is generally assumed that the deformation and deterioration of marble depends on a combination of intrinsic and extrinsic factors. The magnitude and orientation of bowing differ widely for the same marble type (see Fig. 5). When considering the north facade of the Oeconomicum Building, all extrinsic and most intrinsic factors are comparable. The influence of temperature and moisture, the effect of fixing systems and the building physics are more or less identical. The only difference is the orientation of the macroscopic foliation with respect to the panel surface, which suggests that slabs of

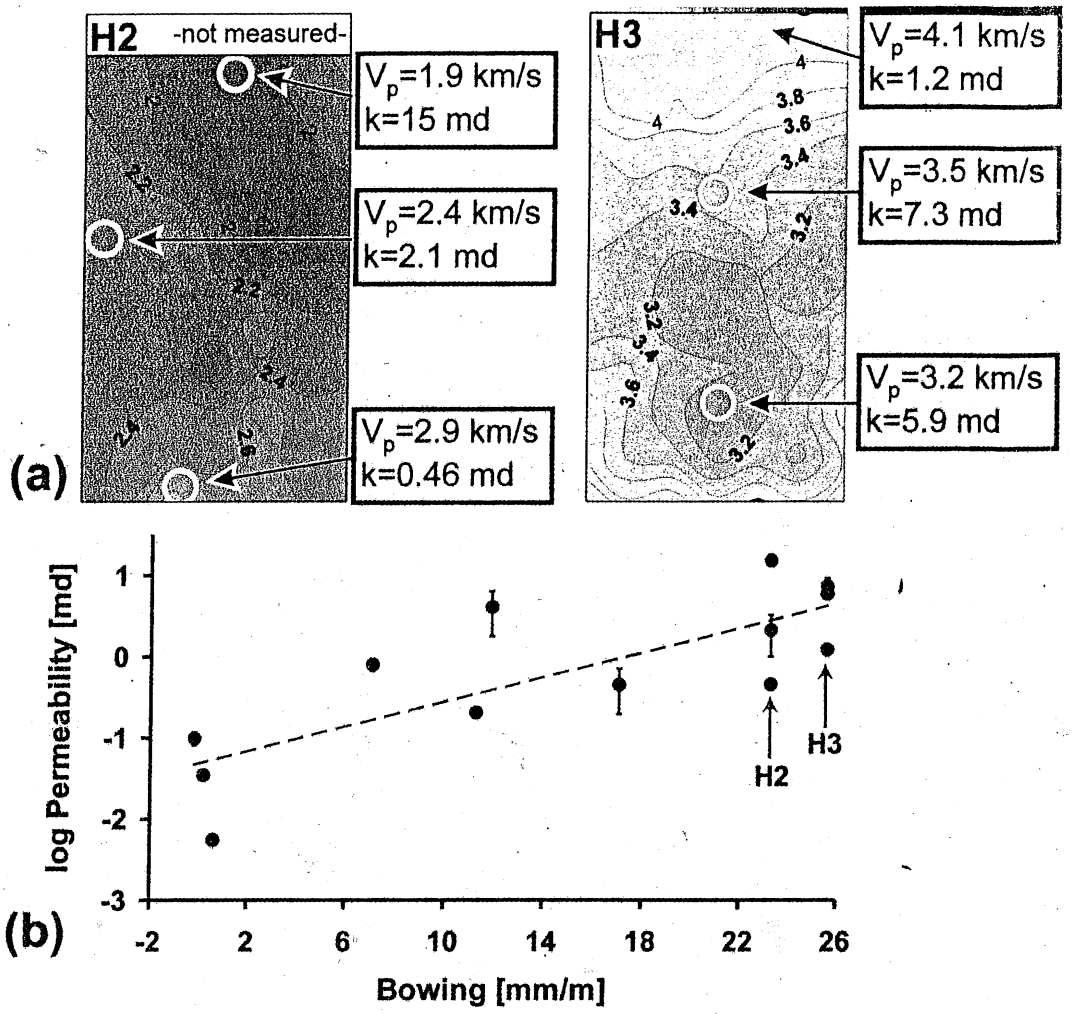

Fig. 13. (**a**) Comparison of ultrasonic velocity (V_p) and permeability (k) for panel H2 and H3. (**b**) Correlation between permeability (logarithmic scale) and deformation (concave bowing). The regression line (dashed) is given. The standard deviations are indicated by error bars. The permeability of panels H2 and H3 is given for three different measuring points (compare with (a)).

marble were cut in various orientations from larger quarry blocks (see Fig. 6). It is assumed that for aesthetic reasons panels with the same decorative elements were combined to form a group of four panels.

To understand the bowing, the microfabric of the strongly deteriorated Peccia marble was examined. The marble is characterized by a large grain size distribution, i.e. from medium to coarser grained (Fig. 14). The medium grain size is between 1 and 2 mm with a maximum of up to 6 mm. Domains with a coarser grain size exhibit a polygonal to interlobate shape, and straight to slightly curved grain boundaries (Fig. 14c). Less coarse grain size domains show an interlobate to sometimes amoeboid grain boundary geometry, where bulging frequently occurs, suggesting grain boundary migration as the predominant mechanism (Fig. 14a,b). More evidence of crystal-plastic deformation is presented by deformation twins and undulous extinction. Furthermore, the fabric is characterized by a preferred grain boundary orientation more or less parallel to the foliation (Fig. 14b,d). In thin sections from strongly bowed panels, open grain boundaries, which are frequently interconnected to intergranular microcracks, can be observed (Fig. 14d). Intracrystalline cracks along twin planes are more rare.

Quantified rock fabrics and their effects on physical properties may contribute significantly to the understanding of rock weathering. Thus, the crystallographic preferred orientation of calcite was measured. The texture was

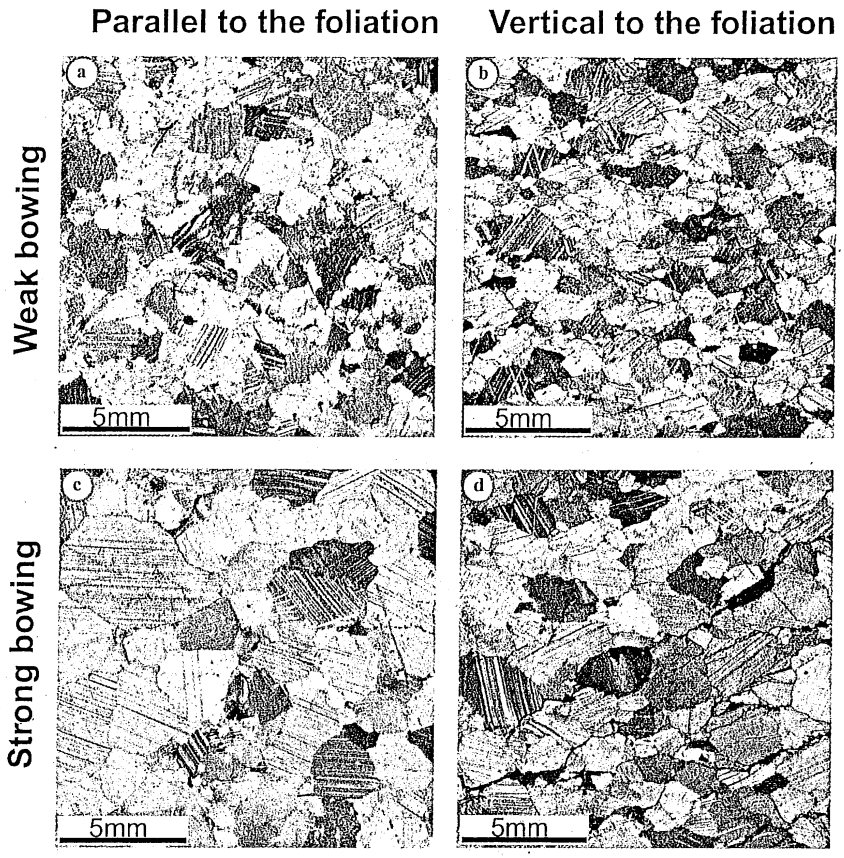

Fig. 14. Representative thin section images (crossed polarizers) from the demounted panels: (**a**) section parallel to foliation, weak bowing; (**b**) section vertical to foliation (horizontal to image plane), weak bowing; (**c**) section parallel to foliation, strong bowing; (**d**) section vertical to foliation (horizontal to image plane), strong bowing.

measured via neutron diffraction and quantified by simple mathematical operations (e.g. Siegesmund & Dahms 1994). The (006) pole figure (Fig. 15a) of calcite shows an intensity maximum normal to the foliation with a weak tendency to form a girdle distribution around the foliation plane, while the (110) poles are arranged on a great circle around the (006) pole density maximum (Fig. 15b). The crystallographic a-axes corresponding to the (110) poles are orientated within the foliation plane. The maximum intensity of 3.6 mrd (multiples of random distribution) of (006) indicates a strong texture (Fig. 15a) and consequently a pronounced anisotropy of the physical rock properties. The importance of calcite textures to the contribution of physical weathering due to thermal treatment has been quantitatively shown by Siegesmund *et al.* (2000) and more extensively by Zeisig *et al.* (2002). A general observation is that the maximum deterioration is closely linked to the c-axis maximum. The coefficient α of calcite is extremely anisotropic (Kleber 1959): $\alpha_{11} = 26 \times 10^{-6}\,K^{-1}$ parallel and $\alpha_{22} = \alpha_{33} = -6 \times 10^{-6}\,K^{-1}$ perpendicular to the crystallographic c-axis, i.e. calcite contracts normal to the c-axis and expands parallel to the c-axes during heating, while the opposite holds true when cooling.

To discuss these effects more quantitatively, preliminary results obtained for Rosa Estremoz marble may be used. Both marbles, Peccia and Rosa Estremoz, are comparable with respect to the lattice and shape preferred orientation (Fig. 15a,c) as well as in their grain boundary geometry. The thermal expansion behaviour was measured on cuboids (10 mm × 10 mm × 50 mm) parallel and normal to the c-axis and a-axis maxima as a function of temperature in the range between 20°C and 80°C (Fig. 15d). The thermal expansion of the samples is extremely anisotropic. As a result of the strong texture (Fig. 15c), a distinct elongation parallel to the c-axis maximum and a more or less constant value parallel to the a-axis concentration can be observed. Systematic measurements on marble reveal that heating and cooling lead to a loss of cohesion along grain boundaries (e.g. Sage

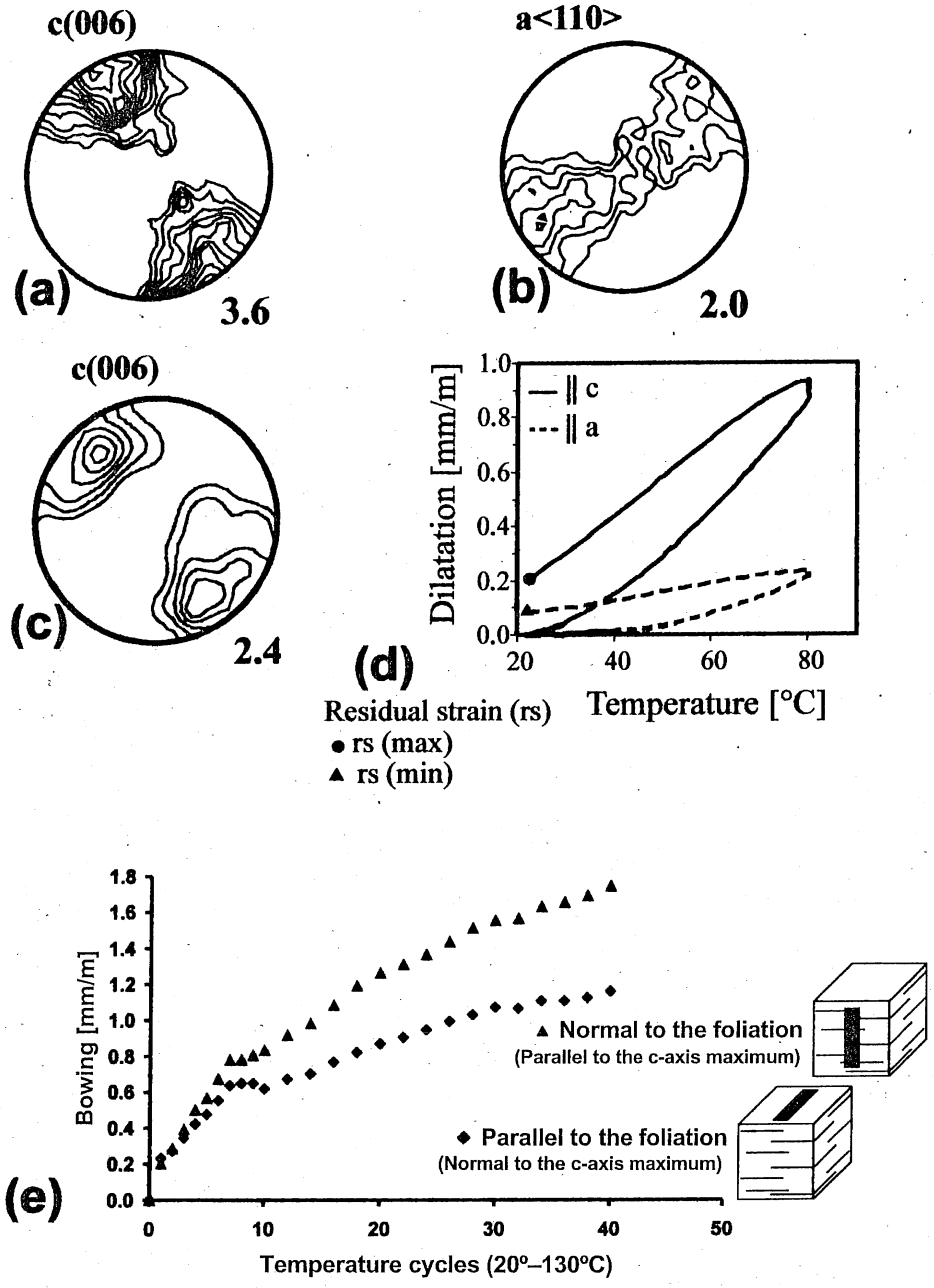

Fig. 15. Correlation between lattice preferred orientation, directional dependence of thermal dilatation and bowing velocity of marble. (**a**) Pole figure of the basal (006) planes of the Peccia marble. (**b**) Pole figure of the a <110> axis of the Peccia marble. (**c**) Pole figure of the basal (006) planes of the Rosa Estremoz marble: lower hemisphere; stereographic projection; lowest contour is equal to 1.0 multiples of random distribution; the relative maxima are given. (**d**) Experimentally determined thermal dilatation as a function of temperature given for Rosa Estremoz marble. (**e**) Bowing of Rosa Estremoz marble versus number of heating cycles (20–130°C). Each curve represents the mean bowing trend of three slabs (400 mm × 100 mm × 30 mm), taken from two different cut-directions with respect to the foliation.

1988; Franzini *et al.* 1984; Zeisig *et al.* 2002). A measurable quantity of the corresponding internal destruction of a marble is the residual strain, i.e. a permanent length change. The residual strain after one heating–cooling cycle of Rosa Estremoz varies between 0.2 mm/m and 0.1 mm/m (Fig. 15d). The effect of the thermal degradation can be easily recognized in the

Peccia marble, since most grain boundaries are open and interconnected to intergranular cracks (Fig. 14d).

The bowing potential of Rosa Estremoz was tested in the laboratory. The test was performed in such a way that the marble specimen (slab of 400 mm × 100 mm × 30 mm) was exposed to moisture on one side and infrared heating on the reverse side. The applied temperature ranged between 20°C and 130°C, and a total of 40 cycles was performed. The difference between both applied approaches was that in the bowing test the effect of moisture is also considered. From dry experiments it is well known (e.g. Battaglia *et al.* 1993) that after some heating cycles (not more than three to five cycles usually) the residual strain will not increase any more, while in the second approach, which includes moisture, the deterioration may increase progressively leading to the bowing effect. The continuous length changes with the applied cycles is clearly documented in Figure 15e. Again, two different samples were used with the same orientation as for the dry thermal treatment (see Fig. 15d). The deterioration rate is different and much faster for samples parallel to the c-axis maximum (1.7 mm/m), whereas perpendicular to these orientations a residual strain of 1.1 mm/m after 40 cycles occurred.

The thermal and/or moisture induced loss of cohesion along grain boundaries or the formation of microcracks is responsible for the increase in porosity with progressive bowing (Fig. 10). Consequently, the increase in permeability clearly indicates that the newly formed pore spaces developed an interconnected network which is supported by the increase in permeability at zones of more pronounced bowing (Fig. 13). Additionally, the reduction in the ultrasonic wave velocities in geometry and magnitude is strongly correlated with the deterioration (Fig. 12). The same observation can be drawn from the decrease in flexural strength (Fig. 11). All vectored physical properties are strongly dependent on direction as a function of the rock fabric.

The detailed observations presented here confirm most of the results that can be found in the literature. Moreover, this study shows that in addition the rock fabric is a very important parameter, when the degree of bowing and the loss in strength are discussed in terms of risk analysis. Caution is needed when trying to correlate the bowing without any fabric considerations. The effect of the rock fabric, especially the lattice preferred orientation, clearly contributes to the deterioration of marbles and finally the degree of bowing. However, this experimental approach cannot explain the processes which determine concave and convex bowing behaviour.

The help of A. Hüpers, C. Müller and G. Maslowski is gratefully acknowledged. We would also like to thank B. Grelk for comments and unreserved discussion. Careful review by T. Yates and G. Ashall is thankfully appreciated. S. Siegesmund thanks the German Science Foundation for a Heisenberg Fellowship.

References

BATTAGLIA, S., FRANZINI, M. & MANGO, F. 1993. High sensitivity apparatus for measuring linear thermal expansion: preliminary results on the response of marbles. *Il Nuovo Cimento*, **16**, 453–461.

BORTZ, S. A., ERLIN, B. & MONK, C. B. 1988. Some field problems with thin veneer building stones. *In*: *New Stone Technology, Design and Construction for Exterior Wall Systems*. American Society for Testing and Materials, Philadelphia, Special technical publication **996**, 11–31.

BUCHER, W. H. 1956. Role of gravity in orogenesis. *Bulletin of the Geological Society of America*, **67**, 1295–1318.

EN 12372, 1999. *Determination of flexural strength under concentrated load*. Deutsches Institut für Normung e.V., Berlin.

FRANZINI, M., GRATZIU, C. & SPAMPINATO, M. 1984. Degradazione del marmo per effetto di variazioni di temperatura. *Rendi conti della Società Italiana di Mineralogia e Petrologia*, **39**, 47–58.

GRIMM, W.-D. 1994. „. . . zum Steinerweichen" – Verformung von Marmorplatten auf alten Friedhoefen. *Naturstein*, Ulm, **10/94**, 52–57.

GRIMM, W.-D. 1999. Observations and reflections on the deformation of marble objects caused by structural breaking-up. *Zeitschrift der Deutschen Geologischen Gesellschaft*, Stuttgart, **150**(2), 195–235.

KLEBER, W. 1959. *Einführung in die Kristallographie*. VEB Technik, Berlin.

LOGAN, J. M. , HADEDT, M., LEHNERT, D. & DENTON, M. 1993. A case study of the properties of marble as building veneer. *International Journal of Rock Mechanics, Mining Sciences & Geomechanics*, **30**, 1531–1537.

RITTER, H. 1992. Die Marmorplatten sind falsch dimensioniert. *Stein*, **H.1/1992**: 18/19.

ROSENHOLTZ, J. L. & SMITH, D. T. 1949. Linear thermal expansion of calcite, var. Iceland spar, and Yule Marble. *The American Mineralogist*, **34**, 846–854.

SAGE, J. D. 1988. Thermal microfracturing of marble. *Engineering Geology of Ancient Works and Historical Sites*, 1013–1018.

SIEGESMUND, S. & DAHMS, M. 1994. Fabric-controlled anisotropy of elastic, magnetic and thermal properties of rocks. *In*: BUNGE, H. J., SKROTZKI, W., SIEGESMUND, S. & WEBER, K. (eds) *Textures of Geological Materials*. Oberursel (DGM Informationsgesellschaft), 353–379.